Comput Geosci (2010) 14:483–502
DOI 10.1007/s10596-010-9178-2

ORIGINAL PAPER

Comparison of numerical methods for simulating strongly nonlinear and heterogeneous reactive transport problems—the MoMaS benchmark case

Jérôme Carrayrou · Joachim Hoffmann · Peter Knabner · Serge Kräutle · Caroline de Dieuleveult · Jocelyne Erhel · Jan Van der Lee · V. Lagneau · K. Ulrich Mayer · Kerry T. B. MacQuarrie

Received: 15 September 2009 / Accepted: 3 February 2010 / Published online: 2 March 2010

Abstract Although multicomponent reactive transport modeling is gaining wider application in various geoscience fields, it continues to present significant mathematical and computational challenges. There is a need to solve and compare the solutions to complex benchmark problems, using a variety of codes, because such intercomparisons can reveal promising numerical solution approaches and increase confidence in the application of reactive transport codes. In this contribution, the results and performance of five current reactive transport codes are compared for the 1D and 2D subproblems of the so-called easy test case of the MoMaS benchmark (Carrayrou et al., Comput Geosci, 2009, this issue). This benchmark presents a simple fictitious reactive transport problem that highlights the main numerical difficulties encountered in real reactive transport problems. As a group, the codes include iterative and noniterative operator splitting and global implicit solution approaches. The 1D easy advective and 1D easy diffusive scenarios were solved using all codes, and, in general, there was a good agreement, with solution discrepancies limited to regions with rapid concentration changes. Computational demands were typically consistent with what was expected for the various solution approaches. The differences between solutions given by the three codes solving the 2D problem are more important. The very high computing effort required by the 2D problem illustrates the importance of parallel computations. The most important outcome of the benchmark exercise is that all codes are able to generate comparable results for problems of significant complexity and computational difficulty.

Keywords MoMaS · Benchmark · Code intercomparison · Numerical methods for reactive transport · Direct substitution approach (DSA) · Differential and algebraic equations (DAE) · Sequential iterative approach (SIA) · Sequential noniterative approach (SNIA)

J. Carrayrou (✉)
Institut de Mécanique des Fluides et des Solides,
Laboratoire d'Hydrogéologie et de Géochimie
de Strasbourg, University of Strasbourg,
UMR 7517 UdS-CNRS, Strasbourg, France
e-mail: carrayro@imfs.u-strasbg.fr

J. Hoffmann · P. Knabner · S. Kräutle
Department of Mathematics, University
of Erlangen-Nuremberg, Erlangen, Germany

C. de Dieuleveult · J. Erhel
INRIA Rennes, Campus de Beaulieu, 35042 Rennes, France

C. de Dieuleveult
ANDRA, Parc de la Croix-Blanche,
92298 Châtenay-Malabry, France

J. Van der Lee · V. Lagneau
Mines ParisTech, 35 rue Saint Honoré,
77305 Fontainebleau Cedex, France

K. U. Mayer
Department of Earth and Ocean Sciences, University
of British Columbia, Vancouver, BC, Canada
e-mail: umayer@eos.ubc.ca

K. T. B. MacQuarrie
Department of Civil Engineering, University
of New Brunswick, Fredericton, NB, Canada, E3B 6E8
e-mail: ktm@unb.ca

1 Introduction

Modeling reactive transport in porous media requires the solution of a coupled set of equations describing the transport of mobile chemical species together with a variety of geochemical reactions [43]. Since initiation of research in this field, reactive transport modeling has been recognized as a problem that may lead to significant mathematical and numerical difficulties. These difficulties originate from numerous challenges related to the solution of each operator (i.e., transport and chemistry) and the coupling of the operators used to evaluate the transport and reaction phenomena. As a result, a body of literature is developing that is devoted to the verification and validation of reactive transport models. In addition, several authors have conducted studies focusing on the performance assessment of reactive transport models and related solution methods. One can distinguish between four cases for these studies:

- Method evaluation based on theoretical considerations
- Comparisons of numerical results with exact or quasiexact solutions
- Intercomparisons of results obtained from two or more numerical methods
- Validation of numerical models based on comparing simulation results with experimental data

A key paper based on theoretical comparisons of solution approaches was presented by Yeh and Tripathi [54]. In this paper, the methods for coupling transport and chemistry were studied, and sequential and global methods were compared with respect to memory requirements and computing time, and calculations were performed based on estimates of the number of unknowns and the number of operations associated with each method. The literature devoted to the evaluation of errors on transport–chemistry (T–C) coupling follows a similar approach. In several contributions (e.g., Valocchi and Malmstead [47], Kaluarachchi and Morshed [20], Barry et al. [2, 3], Leeming et al. [24], Kanney et al. [21], Carrayrou et al. [9]), a variety of methods were evaluated by comparing mass balances obtained using the sequential approaches with exact mass balances.

Numerous verification studies have been performed by comparing numerical and exact analytical solutions. Unfortunately, the problems handled by analytical solutions are highly simplified and do not allow a full evaluation of the capabilities of multicomponent reactive transport codes. Available analytical solutions are typically restricted to 1D transport of a single species in homogeneous media (e.g., Van Genuchten and Wierenga [49], Selim and Mansell [38], Van Genuchten [48], Carnahan and Remer [5]). Some studies deal with 2D and 3D transport [45], and a few attempts have been made to include more complex chemical reaction networks. For example, Toride et al. [46] considered a two-site sorption model present in both mobile and immobile domains. However, analytical solutions are generally limited to homogeneous and unidirectional flow fields, and the geochemical system involves only one or two reactions described either by isotherms or by first-order rate expressions. In reality, flow systems are not restricted to one spatial dimension but may require 2D [14] or 3D [18] spatial discretizations, often further complicated by physical and chemical heterogeneities [4] or fractures [30]. The chemical reaction network may include instantaneous equilibrium reactions [53], kinetic processes [37], or a mixed reaction network (e.g., Mayer et al. [27]), subject to a high degree of coupling and nonlinearity. Processes may include mineral weathering and formation [25], biological phenomena [32], radioactive decay [15], competitive sorption and ion exchange [44], and isotope fractionation [33] and may involve more than 200 chemical species (e.g., Bain et al. [1]).

Model validation can be attempted by comparing numerical results with experimental data. For example, van Genuchten et al. [50] evaluated a reactive transport model based on experimental data that describes transport and nonlinear sorption of trichlorophenoxyacetic acid. Validation of reactive transport models is an important task; however, the a priori verification of the numerical code is still required because it needs to be demonstrated that the numerical code solves the governing equations correctly and accurately. Comparisons of simulation results to experimental data alone do not provide a suitable tool for model verification. This approach does not allow distinguishing between differences that are due to an incorrect implementation of the governing equations, discrepancies associated with an incomplete or faulty conceptual model, or deviations associated with experimental and analytical uncertainties.

Based on these limitations, a suitable avenue for model verification appears to be the intercomparison of numerical results. This intercomparison involves the independent solution of the same problem using a variety of models and/or numerical techniques. One of the main advantages of this method is that complex systems that are more representative of real world reactive transport problems can be considered. The intercomparison of numerical results also has some disadvantages, specifically that the *true* solution of the problem

is not known; however, obtaining the same or very similar results with a variety of computer codes, which are based on different methods and implementations, provides increased confidence in the accuracy of the codes and the field of reactive transport modeling in general.

Despite these obvious benefits, very few model intercomparisons have been published to date. Freedman and Ibaraki [17] compared different solution approaches to model redox processes by comparing the two codes DYNAMIX and DART. De Windt et al. [14] present an intercomparison of the reactive transport codes CASTEM, CHEMTRAP, PHREEQC, and HYTEC for the simulation of oxidation, dissolution, and transport of uranium. The intercomparison presented by De Windt et al. [14] involves a relatively complex chemistry geochemical system and a 2D flow field. In addition, there are very few comparisons that provide information about the performance of the numerical methods used. The literature devoted to the comparison of sequential and global approaches for T–C coupling [13, 16, 35, 36, 39, 42, 43] provides some discussion that is mostly qualitative in nature. Reeves and Kirkner [34] provide the computing times required for the solution of a 1D problem with sorption of one, two, or three components for a number of methods. In these studies, comparisons are typically based on the same mesh size and/or the same time step, despite the fact that each method requires its own time step and mesh size.

Hence, the literature devoted to comparison of numerical solutions for reactive transport models is subject to some limitations, such as

- low degree of complexity
- lack of performance evaluation
- low number (two or three codes) of simultaneous comparisons

The reactive transport benchmark of MoMaS has been designed to help fill these gaps. The benchmark provides a high degree of complexity and nonlinear coupling and provides a platform that allows focusing on the comparison of methods and implementations by ensuring that all participants use the same model. The reaction network is synthetic in nature, removing the dependence on the formulation of activity corrections or database dependencies. Results are thus strictly identical from a chemical perspective. The objectives of this benchmark are then to compare the numerical methods and their implementations.

The first objective is to analyze the ability of the different methods to solve the various benchmark tests. We investigate three classes of numerical coupling: sequential noniterative approach (SNIA) based on transport operator splitting and no iteration between transport and chemistry, sequential iterative approach (SIA) based on an implicit scheme and fixed-point iterations for nonlinear coupling of transport and chemistry, and global methods based on an implicit scheme and Newton iterations for nonlinear coupling. We do not investigate SNIA methods based on an explicit scheme.

The second objective is to provide a measure for computational efficiency. Twenty years ago, Yeh and Tripathi [54] concluded that "Those models that use the DAE approach or the DSA require excessive CPU memory and CPU time. They can only remain as a research tool for one-dimensional problems." We design challenging 1D and 2D test cases in order to check if modern, global approaches can compete with sequential approaches. We compare three implementations of the global approach, which differ by the number of coupled unknowns, in order to measure the impact of a reduction of unknowns. The efficiency is strongly related to the numerical coupling but also to the discretization schemes, to the solution algorithms, and to the implementation. For example, various strategies have been implemented to control the time step and to control the convergence of nonlinear iterations. We do not aim at ranking the methods and the codes. Indeed, the conclusions are valid only for the test cases used, some of the codes are still under development, and the computers used are not the same. Despite these limitations, we attempt to draw conclusions regarding performance of the methods with general relevance.

The third objective is to provide a measure for the accuracy of the numerical results. The comparison must be global but must also highlight some local key features such as a peak of concentration. Accuracy can be analyzed qualitatively by using, for example, visualization tools. In order to derive a quantitative measure, it is necessary to define a reference solution. Again, we try to draw some general conclusions, based on the results of the test cases.

This paper presents results from five different research teams using five different approaches: SNIA with operator splitting, SIA, and three variants of global approaches. This contribution presents a synthesis of the results obtained by the five codes. We use four test cases, from the so-called Easy test case collection of the MoMaS reactive transport benchmark. Additional simulation results for these test cases and other test cases [10] are documented in the contributions by the individual participants [6, 12, 19, 23, 26].

We first describe the reactive transport model used for designing the benchmark. Then, we briefly present the five codes used, along with a short description of their main features. Before presenting the results,

Table 1 Equilibrium table for the easy test case

	X_1	X_2	X_3	X_4	S	K
C_1	0	−1	0	0	0	1.00E−12
C_2	0	1	1	0	0	1
C_3	0	−1	0	1	0	1
C_4	0	−4	1	3	0	0.1
C_5	0	4	3	1	0	1.00E+35
CS_1	0	3	1	0	1	1.00E+6
CS_2	0	−3	0	1	2	1.00E−01
Total (m L^{-3})	T_1	T_2	T_3	T_4	TS	
Initial for medium A	0	−2	0	2	1	
Initial for medium B	0	−2	0	2	10	
Injection $t \in [0; 5{,}000]$	Imposed total concentration at inflow boundary					
Inflow for 1D	0.3	0.3	0.3	0		
Zone 1 for 2D	0.3	0.3	0.3	0		
Zone 2 for 2D	0.3	0.3	0.3	0		
Leaching $t \in [5{,}000; \ldots]$	Imposed total concentration at inflow boundary					
Inflow for 1D	0	−2	0	2		
Zone 1 for 2D	0	−2	0	2		
Zone 2 for 2D	0	−2	0	2		

we describe the methodology used for achieving the objectives of comparison. Finally, we discuss the results and provide some concluding remarks.

2 Reactive transport model

Reactive transport is described using the advection–dispersion equation with reactions subject to the instantaneous equilibrium assumption:

$$\omega \frac{\partial \left(T_{\mathrm{M}_j} + T_{\mathrm{F}_j}\right)}{\partial t} = -\nabla \left(\omega u T_{\mathrm{M}_j}\right) + \nabla \left(\overline{\overline{D}} \times \nabla T_{\mathrm{M}_j}\right) \quad (1)$$

Where t is the time, u is the pore water velocity, T_{M_j} is the total mobile concentration for each component and T_{F_j} is the total immobile concentration. $\overline{\overline{D}}$ is the dispersion tensor, and ω is the porosity. Chemical reactions give the relations between T_{M_j} and T_{F_j} by the way of mass action laws and conservation equations.

The chemical phenomena are summarized in form of an equilibrium tableau in Table 1. The reactions involve four aqueous components and one immobile component, leading to the formation of five aqueous and two adsorbed secondary species. A characteristic of this chemical system is that it contains very high stoichiometric coefficients: from −4 to 4 for component X_2; and equilibrium constants encompassing an extreme range from 10^{-12} for C_1 to 10^{35} for C_5.

One-dimensional and 2D domains were studied. For both cases, the domains are heterogeneous both in terms of hydrodynamic and chemical properties (see Fig. 1). The domains are composed of two media: Medium A is highly permeable, with low porosity and low reactivity, whereas medium B has a low permeability with high porosity and high reactivity. A complete

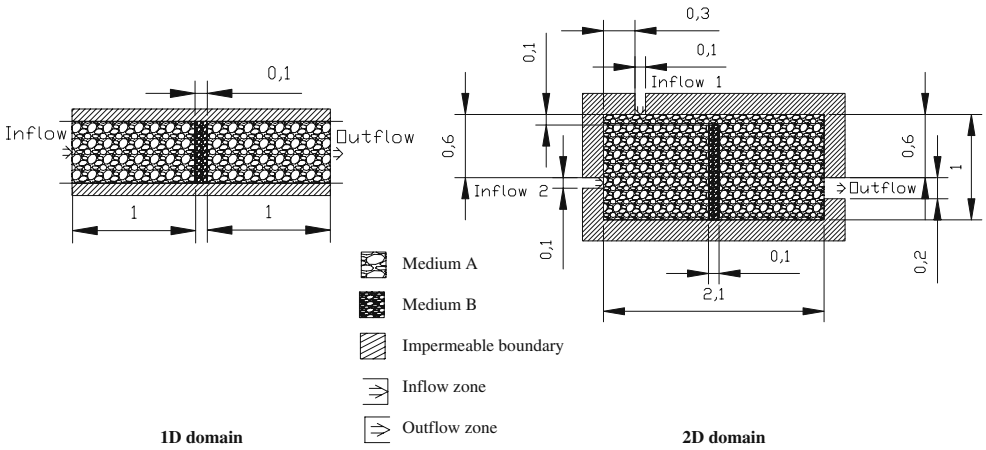

Fig. 1 Scheme of the 1D and 2D domains

description of the exercise can be found in Carrayrou et al. [10].

3 Numerical methods and codes

Brief summaries of the key features of the codes used by the benchmark participants are presented below with a focus on the most significant differences between implementations. Table 2 provides an overview of the key characteristics of the codes: The first row entries describe the method of coupling between transport and chemistry operators; the second row entries introduce the formulation for advection and dispersion operators; the third row entries describe the method used for spatial discretization; the fourth row entries represent the time discretization used; in the fifth row, the method used to linearize the chemical system is provided; the sixth row entries describe the convergence criteria used for linearization (all criteria have been tested and chosen sufficiently small to have no influence on the accuracy of the proposed solutions); and the last row represents the method used for the solution of the linearized system of equations. For a more detailed description of the codes, we refer to the individual articles in this special issue. Although this work is devoted to a comparison of numerical methods implemented in the participating reactive transport codes, the general capabilities of the codes are presented for completeness and to provide additional perspective (Table 3).

3.1 GDAE1D

This code is based on a method of lines in combination with a global approach in order to solve the partial differential algebraic equations (DAE) involving transport and chemistry [12, 13]. In the current version, spatial discretization is achieved by a classical finite volume method, with upwinding for advection and centered spatial discretization for dispersion. The design of the mesh uses constant spatial discretization intervals. The resulting DAE are solved by an external, robust, and efficient DAE solver. Time discretization is performed by a multistep implicit scheme: a backward differentiation formula (BDF) with variable order and variable time step. BDF is used in connection with a modified Newton method in order to deal with nonlinearity. The sparse linear systems are solved by a direct method, a multifrontal Gaussian elimination with pivoting. Symbolic factorization and renumbering for fill-in reduction are performed once by using the matrix structure. Due to the connection between BDF and Newton's method, the Jacobian matrix is updated only when necessary and the time step is controlled to ensure both convergence of Newton's method and the accuracy of the scheme. The main computational cost is associated with the factorization of the Jacobian matrix and the solution of the triangular system of equations. For large computational domains, it is necessary to decrease the computational cost. Several issues will be addressed in future versions: the spatial grid will be nonuniform; the tolerance thresholds in the DAE solver will be tuned; and the substitution approach will be applied in the linear system in order to reduce the number of unknowns. For the benchmark exercise, 600 cells were used for the 1D advective case, while 400 cells were used for the 1D dispersive case. Small tolerance thresholds were specified to the DAE solver.

3.2 Code of Hoffmann et al.

This solution method reduces the size of the nonlinear system and, thus, the required computational resources. The system of equations, consisting of partial (PDEs) and ordinary differential equations (ODEs) for the mobile and immobile species and nonlinear advection equations (AEs) describing local equilibria, is transformed by (a) taking linear combinations between the differential equations, (b) the introduction of a new set of variables, i.e., a linear variable transformation, and (c) the elimination of some of the new variables by substituting local equations, such as AEs and ODEs, into the PDEs. Application of (a) and (b) leads to a decoupling of the linear PDEs; this decoupling in combination with (c) leads to a reduction of the size of the nonlinear system (see Kräutle and Knaber [22], Hoffmann et al. [19], and the references therein for details). The system of equations is handled in the spirit of a global implicit approach (one-step method) and avoids operator splitting. However, the substitution of the local equations does not, as is the case for other direct substitution approaches, destroy the linearity of the transport term. The algorithm was implemented using a software kernel for parallel computations involving PDEs, called "M++." M++ itself is an object oriented code based on C++. The code is implemented for 2D problems and uses finite elements on unstructured grids. The nonlinear system of equations is linearized using Newton's method and solved using a preconditioned BiCGStab algorithm. For the solution of the flow problem, mixed hybrid finite elements are used. For the flow computation in the 2D case of this benchmark, Brezzi-Douglas-Marini elements of order one were used. This method guarantees an accurate solution of the flow problem despite the significant permeability contrast between the two media. To facilitate

Table 2 Summary of the main features of the compared codes

Method	SPECY	HYTEC	MIN3P	Hoffmann et al.	GDAE1D
Transport–chemistry coupling	SNIA no iteration	SIA fixed-point iterations	DSA	Reduced-global ODE approach	DAE
Advection–dispersion OS	Yes	No	No	No	No
Spatial discretization	Discontinuous finite element for advection and mixed finite element for dispersion	Finite volume and Vornoï mesh	Finite volume, upwinding, centered, or flux limiter for advective term	Finite element and finite volume upwinding	Finite volume upwinding
Time discretization	Explicit for advection implicit for dispersion and constant time step	Implicit adaptive time step	Implicit adaptive time stepping	Implicit adaptive time step	Implicit adaptive order adaptive time step
Linearization	Chemistry only: Positive continuous fraction as preconditioner and Newton–Raphson with restricted search domain	Chemistry only: Newton–Raphson with relaxation factor	Modified Newton substitution of variables	Newton reduction of variables and substitution	Newton no substitution
Convergence criteria	For chemistry only: Relative error on mass balance of 10^{-12}	Relative criteria on fixed concentration of 10^{-8}	Relative criteria on concentration update: relative error of $\Delta \ln c < 10^{-8}$	Relative and absolute criteria on the residual of Newton's method. Relative error of 10^{-6}. Residual of 10^{-10}	
Resolution of linear systems	Direct multifrontal solver	Preconditioned GMRES	Preconditioned BiCGStab algorithm	Preconditioned BiCGStab algorithm	Direct method, a multifrontal Gaussian elimination with pivoting

Table 3 Summary of the main phenomena and models included into the compared codes

Phenomena	SPECY	HYTEC	MIN3P	Hoffmann et al.	GDAE1D
Flow field	No, calculated separately	Constant or transient, unsaturated (Richards equation)	Yes	Constant or calculated by solving Richards equation	No
Unsaturated flow	No	Yes	Yes	Yes	No
Multiphase flow	No	No	No	Implementation in progress	No
Gas phase transport	No	No	Yes	No	No
Variation of porosity	No	Yes	Yes	No	No
Aqueous-gas exchange	Henry's law, included into mass action laws	Henry's law, included into mass action law	Yes	Phase diagrams given following molar fractions	No
Activity correction	Debye–Hückel Güntelberg Davies	Debye–Hückel, extended Debye–Hückel, Davis, B-dot, SIT	Extended Debye–Hückel Davis Pitzer	No	No
Precipitation dissolution	Yes Instantaneous equilibrium and kinetic	Yes Equilibrium and kinetic	Yes Kinetic formulation	Yes. instantaneous equilibrium and kinetic, using formulation with complementarity condition	No
Ion exchange	Yes	Yes	Yes	Yes	Yes
Surface complexation	Constant capacity model Diffuse layer model Stern model Triple layer model	Constant capacity, diffuse layer, and triple layer models	Nonelectrostatic adsorption model	Sorption according to law of mass action with surface complex No electrostatic correction	Nonelectrostatic adsorption model
Kinetic chemistry	Yes Model to be defined by user	Yes: distance from equilibrium, Monod, energy term, catalysis/ inhibition (all reactions: aqueous, surface or mineral)	Yes (intra-aqueous kinetic reactions and dissolution precipitation)	Yes law of mass action	No
Biologic	Not specific but included into the kinetic module	Specified through kinetic reactions	Can be specified through kinetic reactions	Monod model	No

fair comparison with the other models, the code was run on a single processor.

3.3 SPECY

SPECY uses a noniterative operator splitting scheme for T–C coupling and for advection and dispersion [8]. Each operator is solved independently using specifically tailored methods: advection is solved using discontinuous finite elements [40]; dispersion is tackled with mixed hybrid finite elements; and equilibrium chemistry is solved using a combined algorithm based on the Newton–Raphson technique and the positive continuous fraction method [7]. The key feature of this code is the use of specific methods to solve each part of the reactive transport equation. Solving the advective part using discontinuous finite elements provides an excellent description of very sharp fronts and eliminates numerical diffusion and nonphysical oscillations. Solving the dispersion term with mixed hybrid finite elements provides an exact mass balance for each element of the mesh and allows the use of a nondiagonal dispersion tensor. The algorithm developed for solving the equilibrium chemistry ensures the convergence of the method for all cases and provides fast convergence for most cases. To optimize computational performance, we used the largest time step allowed by SPECY. This constant time step length is determined by a Courant–Friedrich–Levy stability criterion equal to one. The reader is refereed to Carrayrou [6] for additional details on the code formulation and its application to the MoMaS reactive transport benchmark.

3.4 HYTEC

HYTEC is a reactive transport model that integrates a wide variety of features and options that have evolved, after more than a decade of development, to a widely used and versatile simulation tool [51]. Solution capabilities for biogeochemistry are provided by the code CHESS (http://chess.ensmp.fr). The model accounts for many commonly encountered processes including interface reactions (surface complexation with electrostatic correction and cation exchange), precipitation and dissolution of solid phases (minerals and colloids), organic complexation, redox and microbial reactions, etc. All reactions can be modeled using a full equilibrium, a full kinetic, or a mixed equilibrium–kinetic approach. Thermodynamic data are taken from the database developed by the Common Thermodynamic Database Project.

The hydrodynamic module of HYTEC is adapted for hydrodynamic conditions commonly encountered in the laboratory or in the field. The code allows for unsaturated media, variable boundary conditions, sinks, and sources [52]. HYTEC searches for an accurate solution to the multicomponent transport problem using an iterative, sequential, so-called strong coupling scheme. Strong coupling permits variable hydrodynamic parameters as a function of the local chemistry. For example, the porosity of a porous medium reduces after massive precipitation of newly formed mineral phases, which modifies the water flow paths and transport parameters, e.g., diffusion coefficients: HYTEC solves this interdependency accurately, which makes the tool particularly useful for, e.g., cement alteration at long timescales (e.g., storage of wastes and performance assessment).

Application domains of HYTEC are numerous and include soil pollution, acid mine drainage, in situ leaching of copper or uranium, radioactive waste disposal (performance assessment, near- and far-field processes), and storage of greenhouse gases. Other applications concern the evolution and degradation of (geo)materials such as ashes, concrete, and cements; the latter often being simulated by a typical CEM-I cement, but more sophisticated models for cements can be used including sorption on primary or secondary calcium silicate hydrate phases, carbonation, and sulfatation of the material. The strong coupling approach as outlined above makes HYTEC particularly useful for the modeling of long-term leaching of solidified wastes.

Efforts to develop, test, and validate the HYTEC model largely exceed the scope of a single laboratory and the timescale of a Ph.D. thesis. The Reactive Transport Consortium (*Pôle Géochimie-Transport* [PGT], http://pgt.ensmp.fr) is a national research project with the objective of creating a long-term framework for the development of reactive transport models, reference studies, and new application domains. Already operational for several years, the collaborative efforts within the PGT allowed to make considerable progress in the domain of reactive transport modeling.

3.5 MIN3P

MIN3P is designed to simulate general flow and reactive transport problems in variably saturated media for 1D to 3D systems. The flow solution is based on Richard's equation, and transport of solute is simulated using the advection–dispersion equation [28]. Gas transport is by diffusion only in the standard version of the code [28] or by advection and diffusion within the framework of the dusty gas model [31]. Geochemical processes included are aqueous complexation, mineral dissolution–precipitation, intra-aqueous kinetic

reactions, gas dissolution, ion exchange, surface complexation, and linear sorption. All reactions considered in the simulations can be specified through a database. The code has been used for a wide range of applications in the field of contaminant transport (e.g., Mayer et al. [27]) and groundwater remediation (e.g., Mayer et al. [29]). The code was also used for investigation of redox stability in crystalline rock formations that may be considered for deep geologic repositories for nuclear waste [41].

The solution of the governing equations is based on the global implicit method, in which the reaction equations are directly substituted into the transport equations, known as the "direct substitution approach" (DSA) [54]. Spatial discretization is performed using a control volume method with half-cells on the boundary. The code uses implicit time weighting and provides a choice of various spatial weighting schemes for advective transport, including upstream weighting, which was used for the current simulations. The governing equations are linearized using a modified Newton's method with variable time stepping; a sparse iterative solver is used for the solution of the linearized matrix equations (see Mayer and MacQuarrie [26], for additional details). For the easy test case presented here, the code was used without any modifications.

4 Methodology of comparison

In order to interest as many research teams as possible and to extend the applicability of the benchmark to a wide variety of methods, the hydrodynamic flow system has been kept straightforward, with only two media and a simple 1D or 2D geometry. For the same reason, the chemical system has been simplified in the sense that activity corrections have been neglected and that sorption reactions do not include electrostatic correction terms. On the other hand, the benchmark has been designed to ensure a high degree of numerical difficulty: physical and chemical heterogeneities are significant, chemical phenomena are strongly coupled and nonlinear, and concentration gradients induced by external forcing due to changes in boundary conditions are substantial.

In this contribution, we focus on a comparison of the results for the easy test case, both for 1D and 2D computational domains, and for the advective and dispersive scenarios. All the five codes have results for the 1D test cases; on the other hand, only three codes give results for the 2D advective test case and only two codes for the 2D dispersive test case; similar results for the 2D test cases can also be found in de Dieuleveult's Ph.D. thesis [11].

We first measure the computational complexity of the codes; since most of them use an adaptive time step, we only measure the CPU time as a function of the number of cells. The CPU time is specified in terms of a system-independent CPU unit, which is defined in the paper introducing the benchmark exercise [10]. Although the CPU time comparison is intended to provide an objective performance-based measure of model and method applicabilities for the various test cases, this method has some limitations. Some codes are in the process of development (GDAE1D de Dieuleveult and Erhel [12], Hoffmann et al. [19]) and only include a limited chemical reaction network, whereas other programs (SPECY, HYTEC, and MIN3P) can handle general and complex reaction networks; in these codes, chemistry can be specified from a database, not only greatly increasing model flexibility but also generating computational overhead (see Table 3). In addition, providing a measure of the computational effort independent of computing hardware and compiler software is quite difficult. The computational complexity must therefore be considered qualitative. For further information on the variability of CPU times as a function of system parameters, we refer to the contribution of de Dieuleveult and Erhel [12].

In the following, the accuracy of the codes is compared. Since the methods used are different, they require different spatial and temporal discretizations to obtain a solution of the same accuracy. Therefore, CPU as a function of grid size should not be assessed in isolation. We could compare the accuracy of codes by using the same number of cells in all of them. We choose a different strategy and compare the accuracy of codes by using the same normalized CPU time for all of them. Maximum allowed computing times are specified for each test case investigated. For the easy test case presented here, the following maximum CPU units were imposed: 3,500 units for 1D advective case, 2,000 units for 1D dispersive case, 10,000 units for 2D advective case, and 10,000 units for 2D dispersive case. Again, this exercise has some limits, but it provides some useful information.

Since the benchmark is designed for handling complex models, there is no analytical reference solution. Since the test cases are synthetic, there is no experimental reference solution. Therefore, it is difficult to derive a quantitative comparison. For the 1D test cases, reference solutions are calculated using fine grids and small time steps, providing a basis for accuracy measurement. An example of this approach is given by Carrayrou [6]. The validity of these reference solutions has been

controlled by successive mesh and time step refinements and by comparison with refined solution from the other codes. Then, we use the reference solution to define an error criteria based on a L2 norm. The norm (L2) is calculated for the studied species ($C_{\text{calculated}}$) over the interval (noted "L"), which can be either the space domain (x varying from 0.0 to 2.1 in 1D case, x varying from 0.0 to 2.1, and y varying from 0.0 to 1.0 in 2D case) or the simulation time (time from 0.0 to 6,000.0). A relative error or deviation between the solutions can be quantified by the L2 norm, which is defined by Eq. 2:

$$L2 = \sqrt{L \times \sum_{\substack{\text{All the } L \\ \text{discretisation}}} \left[\frac{\Delta L_i}{L} \left(C_{i,\text{calculated}} - \sum_{\substack{\Delta L_i \text{ discretisation} \\ \text{on reference}}} \frac{dL_{j,\text{ref}} \times C_{j,\text{reference}}}{\Delta L_i} \right)^2 \right]} \tag{2}$$

In Eq. 2, ΔL is the discretization used by the calculated solution and $\mathrm{d}L_{j,\text{ref}}$ is the discretization used by the reference solution over ΔL_i.

For the 2D test cases, it was not possible to define a reliable reference solution because computational requirements were too high for a very refined mesh. In order to compute an L2 norm, we used the most refined computation as reference.

This criterion gives a global quantitative comparison of accuracy. However, since there are many species, with concentrations varying in space and time, it is difficult to represent and to analyze all the results. The global quantitative comparison gives some information but does not highlight some local key points. In order to compare the local accuracy of the codes, we select representative results that focus on key difficulties of the benchmark and, at the same time, highlight the most significant differences between the five codes. Thus, we compare the results given by the codes for some specific species at some specific time or location. The purpose of this comparison is to analyze if a code can compute an accurate solution for a specific pollutant or near a pumping well.

5 Results

5.1 Computational complexity

To illustrate the computational complexity of the various codes, we plot the normalized CPU times as a function of the number of cells in the mesh. Results for the 1D advective and dispersive test cases are presented in Figs. 2 and 3, respectively. Results for the 2D advective test case are presented in Fig. 4.

As expected, the computational complexity of all codes is characterized by a linear log–log relationship between CPU time and mesh size, independent of the test case considered. It appears that all codes have the same slope for the 1D test cases (except HYTEC for the 1D advective test case). For the 1D advective and dispersive test cases (Figs. 2 and 3), well-known results are confirmed: the SNIA (SPECY) is faster than other methods, for a fixed number of cells. However, as suggested by Saaltink et al. [35], implementations of the DSA approach (e.g., MIN3P, Hoffmann et al.) can lead to competitive CPU performance. The new reduction scheme developed by Kräutle and Knabner [22] (see also Hoffmann et al. [19]) decreases further the computational complexity. Despite the use of a global approach, this implementation shows equivalent or lower CPU times than required by all other codes. Moreover, it must be underlined that this code uses a 2D discretization to emulate a 1D domain. This method is more CPU time consuming than solving a 1D problem. Global methods appear very competitive for the 2D advective test case. Extrapolating the performance data for each of the three codes in Fig. 4 shows that for a mesh with the same number of cells, the CPU requirements for the code by Hoffmann et al. are more

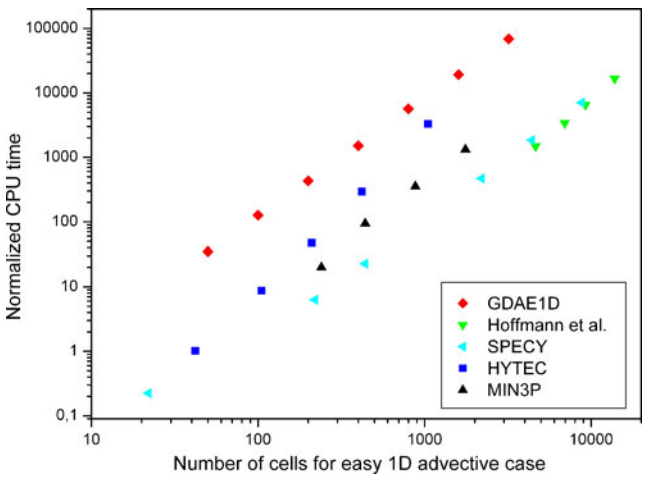

Fig. 2 Normalized computing times as a function of discretization for the 1D easy advective test case

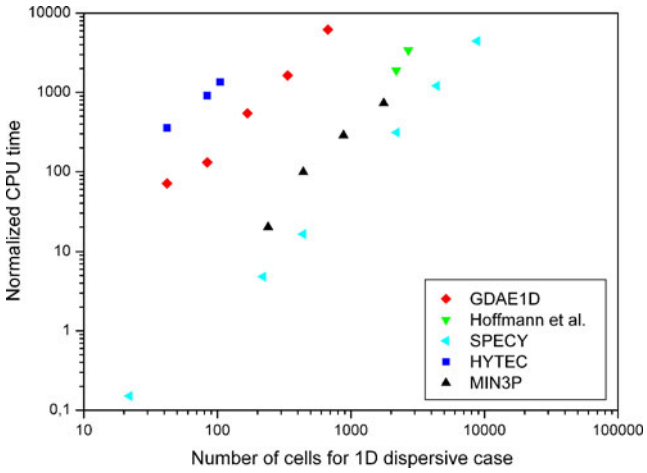

Fig. 3 Normalized computing times as a function of discretization for the 1D easy dispersive test case

than five times lower than the CPU times of the two other codes.

However, we emphasize that this measure does not provide insight for accuracy. So, now we present a comparison of accuracy, with all the codes using approximately the same normalized CPU time.

5.2 Accuracy for 1D easy advective test case

The requirement to limit CPU times to no more than 3,500 CPU units led to a range of spatial discretizations for the various codes. GDAE1D used 600 uniform cells, while HYTEC was run with 1,073 uniform cells. The SPECY and MIN3P simulations were conducted with nonuniform grids. The discretization in the low-permeability zone in the center of the domain (medium B) was refined by a factor of 2; SPECY and MIN3P employed 6,400 and 1,760 cells, respectively. Hoffmann et al. used a 2D discretization to emulate the 1D problem by replacing the 1D computational domain with a narrow 2D domain. A preadapted triangular mesh was used with different grid sizes in the two media: grid size h_1 in medium A and grid size h_2 in medium B with $h_1 = 4h_2$. The resulting mesh consists of 6,942 cells with 1,155 nodes in the x-direction. In medium A, the mesh has three nodes in the y-direction.

A global quantitative comparison between the results given by each code and the reference solution is performed using the L2 error norm (see Table 5). The reference solution is given by SPECY using a 8,200 cells mesh and a constant time step of 1.14×10^{-4}. All the codes provide similar error norms. The best results are obtained by GDAE1D, although the approach chosen by GDAE1D is computationally intensive and requires using a coarse grid to respect the specified CPU time criteria. The results provided by HYTEC leads to the second L2 norm. The results given by the code of Hoffmann et al. and by MIN3P lead to the third and fourth L2 norms.

This global criterion is not sufficient to compare accuracy. To compare local results for this test case, we have selected the concentration profile of the fixed component S at time 10. This profile is characterized by sharp concentration fronts with a very narrow peak located near the inlet of the domain (Fig. 5). This concentration peak is due to the disequilibrium created by the injection of species X_3. The influence of the more reactive medium B can be seen in the center of the domain, as indicated by the higher concentration of S. All codes produce very similar concentration profiles at

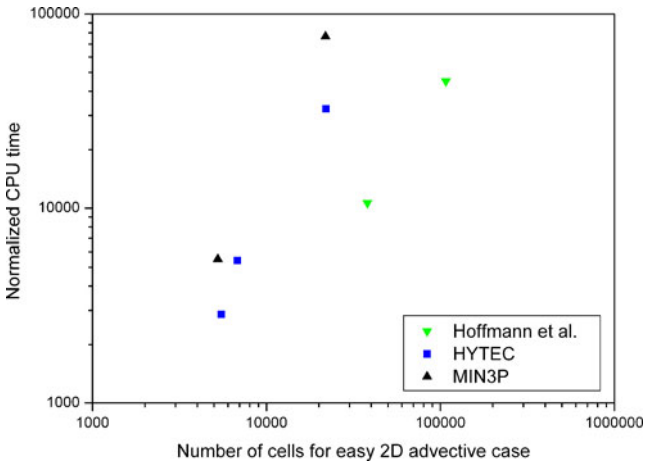

Fig. 4 Normalized computing times as a function of discretization for the 2D easy advective test case

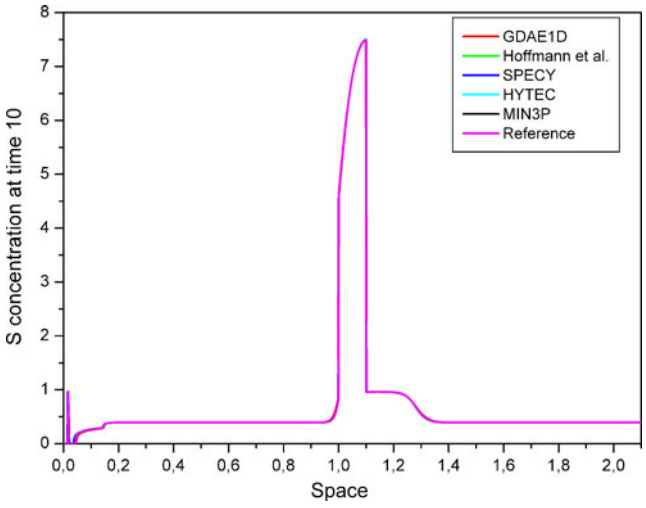

Fig. 5 Concentration profiles of solid component S at time 10 for the 1D easy advective test case

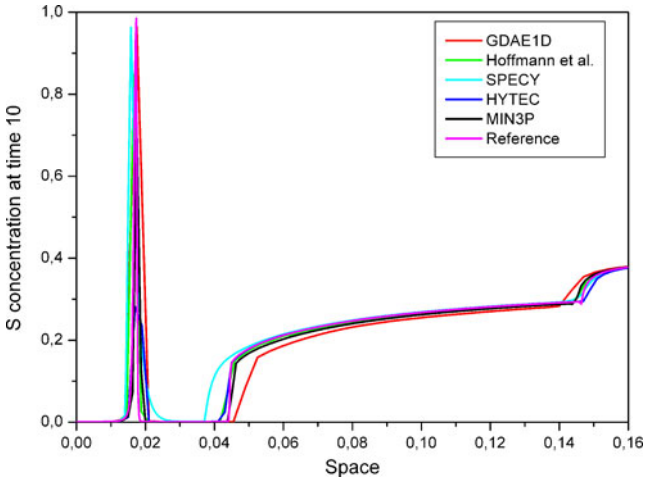

Fig. 6 Local concentration profiles of solid component S at time 10 for the 1D easy advective test case (subregion: $x = 0$ to $x = 0.16$)

the scale of the solution domain. More comprehensive results presented in the individual contributions for each code [6, 12, 19, 23, 26] confirm the good agreement for other chemical species.

However, Fig. 5 also reveals small discrepancies for the concentration peak near the domain inlet. Zooming into this region provides a sensitive measure for a more in-depth code comparison. The location and intensity of the peak at $x = 0.02$ (Fig. 6) provide a direct indication of coupling error or numerical diffusion. Figure 6 indicates that there are indeed small differences in the location of the concentration peak and the magnitude of the peak concentration.

Table 4 provides a quantitative assessment of these differences suggesting that all codes produce similar peak locations with a low standard deviation; however, the maximum concentrations calculated by the various codes are characterized by a wider range. Successive mesh and/or time step refinements performed using the various models indicate that for the exact solution of S, the peak concentration will exceed 0.9 (see Carrayrou [6]). The reference solution is a peak of 0.985.

Table 4 Location and peak amplitude for the first S peak at time 10 for the 1D easy advective test Case

	Location of the peak	S concentration of the peak
GDAE1D	0.0175	0.966
Hoffmann et al.	0.0167	0.852
SPECY	0.0158	0.968
HYTEC	0.0170	0.286
MIN3P	0.0175	0.725
Reference	0.0174	0.985
Mean	0.0169	0.759
Standard deviation	7.04×10^{-4}	0.283

Even if the intensity of the peak is low with HYTEC, its localization is good, and the rest of the curve fits well with the reference solution. Traditionally, one of the main advantages of operator splitting methods is that tailored numerical methods can be used for each operator, including exact transport schemes to minimize numerical diffusion [43]. This is confirmed by the results obtained using SPECY (Fig. 6, Table 4). However, this peak is shifted to the left. Moreover, the curve between $x = 0.04$ and $x = 0.15$ is far from the reference.

The closest peak location and intensity to the reference are computed by GDAE1D. Thus, this global method achieves high peak concentrations despite a relatively coarse discretization. This is probably due to a small error tolerance in the DAE solver, inducing small time steps. It seems to indicate that global methods can be implemented with a low degree of numerical diffusion. For GDAE1D, some differences can be seen on Fig. 6 between $x = 0.04$ and $x = 0.15$; they are probably due to a small number of grid cells.

5.3 Accuracy for 1D easy dispersive test case

For the 1D easy dispersive test case, the maximum normalized CPU time was set to 2,000 CPU units. To meet this criterion, GDAE1D used a uniform discretization with 400 cells, while the HYTEC simulation employed 137 uniform cells. As for the 1D advective case, the SPECY and MIN3P simulations used a nonuniform discretization with grid refinement in medium B (by a factor of 2). For the SPECY simulation, the domain is discretized into 5,800 cells, while the MIN3P simulation was based on a grid with 880 cells. Hoffmann et al. used a narrow 2D computational domain to describe the 1D system. However, unlike the 1D advective case, no grid refinement was performed, and a regular mesh with three nodes in the y-direction was specified. The resulting grid consists of 2,184 triangles with 547 nodes in the x-direction.

L2 error norms are given on Table 5. The reference solution is given by MIN3P using a 1,760 cells mesh and a time step limited to CFL = 1. Again, all codes provide similar norms. Code MIN3P leads to the smallest L2 norm, followed by GDAE1D, then the code Hoffmann et al., finally SPECY and HYTEC. Global approaches are efficient for dispersive problems, and the mesh used by MIN3P is the finest among other global codes.

For this case, local accuracy measurement is based on breakthrough curves for species C_2 at the outflow of the domain (Fig. 7). C_2 concentrations increase rapidly

Table 5 L2 norm for the different test cases calculated versus a reference solution

Case	SPECY	HYTEC	MIN3P	Hoffmann et al.	GDAE1D
1D advective Figure 5 Reference given by SPECY	7.67×10^{-2}	2.54×10^{-2}	5.40×10^{-2}	5.00×10^{-2}	1.75×10^{-2}
1D dispersive Figure 7 Reference given by MIN3P	2.63×10^{-2}	2.89×10^{-2}	1.25×10^{-3}	1.05×10^{-2}	6.92×10^{-3}

after approximately 300 time units, and they equal the composition of the injected solution, followed by a sharp drop due to the change of the inflow boundary condition (after 5,000 time units). The simulation results indicate that all codes consistently reproduce the increase and decrease of the C_2 concentration front (Fig. 7).

This dispersive test case provides a serious test for implementations based on the sequential approach. The short timescale of dispersive transport effectively leads to an increased solute flux with possible feedback on local chemistry from several neighboring cells. These types of problems are known to be prone to the introduction of coupling errors, while global methods are expected to perform well.

This hypothesis is confirmed by the results shown in Fig. 7, which indicate an excellent agreement between the different global approaches (GDAE1D, Hoffmann et al., and MIN3P). Discrepancies between these three codes are particularly small. On the other hand, the SIA and SNIA solutions show slight deviations. Minor differences are visible for the codes using the SIA and SNIA methods during the flushing period (>5,000 time units); however, it must be emphasized that the time frame displayed is less than 5 time units, while the total simulation period is 6,000 time units.

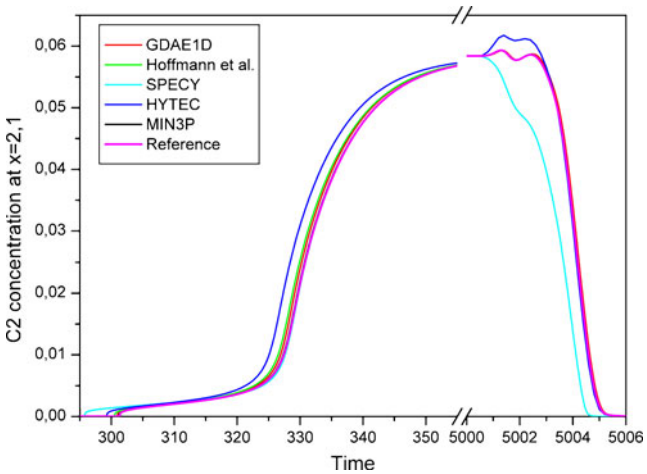

Fig. 7 Elution curve for species C_2 at $x = 2.1$ for the 1D easy diffusive test case

However, solutions obtained for refined grids (e.g., SPECY and Carrayrou [6]) converge toward the results obtained by the global methods, suggesting that errors are reduced by refining space and time.

5.4 Accuracy for the 2D easy advective test case

The 2D version of the easy advective test case was solved using three of the codes (HYTEC, MIN3P, and Hoffman et al.). Again, restricting the CPU time to a maximum of 10,000 units led to different spatial discretizations. Hoffmann et al. used a preadapted mesh with 38,016 triangles, refined in the fast velocity zone and near the outflow. The HYTEC solution used a grid with 8,840 cells (136 × 65) to comply with the CPU criterion. MIN3P employed a grid with 5,250 control volumes (105 × 50).

The concentration contours of component X_3 at time 1,000 offer a suitable means for comparison. Figure 8 clearly depicts high concentrations in the vicinity of the two injection zones, one located on the left boundary and the second located near the top of the model domain. High concentration regions are delineated by sharp fronts controlled by sorption and complexation reactions. In addition, the concentration distributions are significantly affected by the presence of medium B, which induces a deviation of the flow lines and a low concentration zone near the bottom of the domain.

Comparing the results demonstrates that all codes are capable of reproducing the key features of the problem (Fig. 8). Overall, simulation results are similar in terms of the magnitude of concentrations and the location of fronts. The most significant differences are observed in the region of divergent flow downgradient of the low permeability zone (medium B) near the top of the domain (Fig. 8). In addition, some deviations are observed in the low concentration zone within medium B near the bottom of the domain.

In addition to the solutions computed subject to the CPU time limitation, the participants could also submit solutions using finer meshes without CPU time

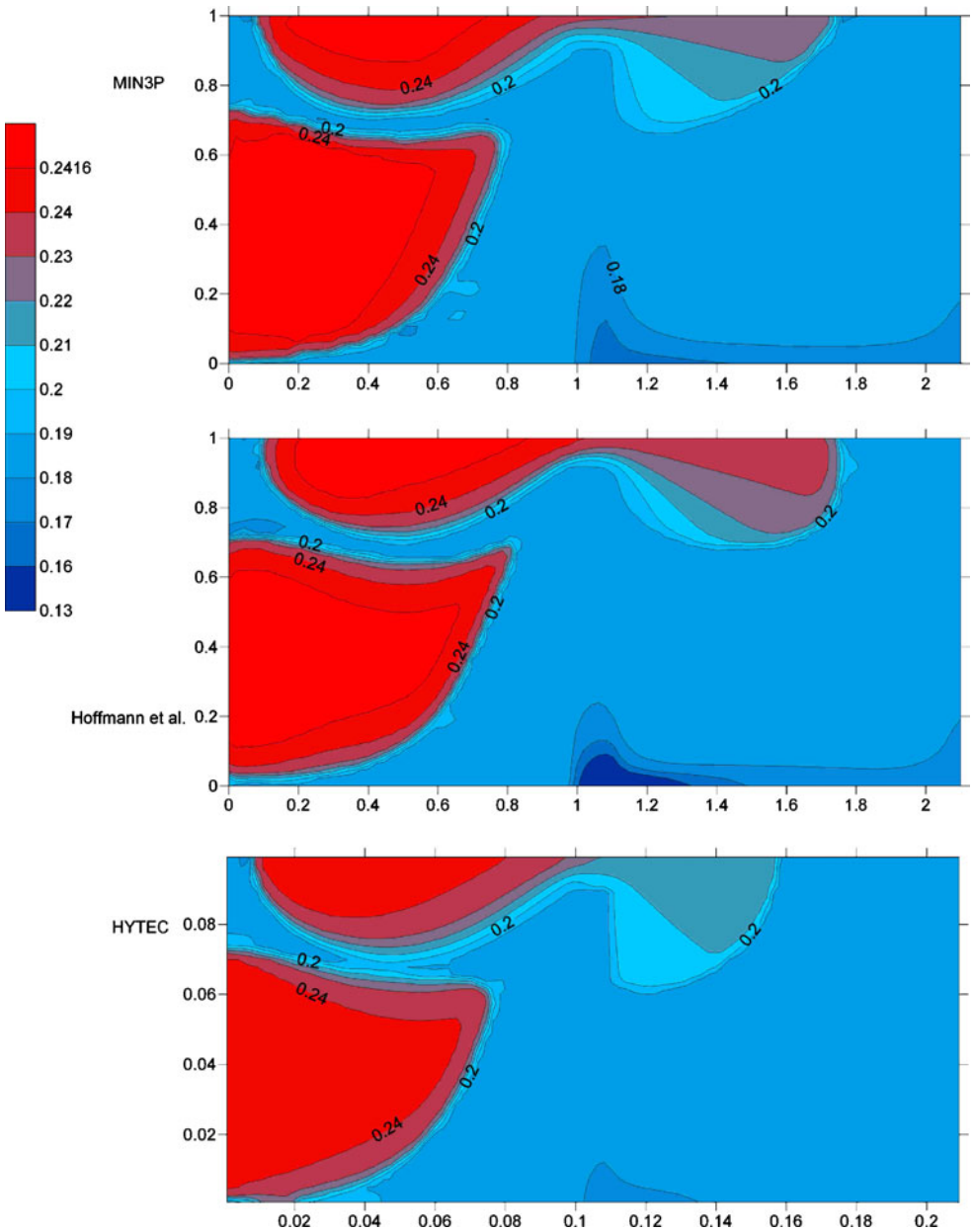

Fig. 8 Concentration contour maps for component X_3 at time 1,000 for the easy 2D advective test case (maximum normalized CPU time is set to 10,000 CPU units)

limitations. In this exercise, Hoffmann et al. used a regular mesh with 107,520 triangles and MIN3P was run with a grid consisting of 21,836 cells (212 × 103). Figure 9 shows the X_3 concentration maps at time 1,000 calculated using these refined meshes. Also, Hoffmann et al. performed a computationally intensive simulation with a 608,256 cells grid, taking 2 weeks on ten processors. The mesh is very fine, and the unstructured mesh used is adapted to describe the meandering flow field. We provide the X_3 concentration map at time 1,000 for this very fine mesh in Fig. 10. The results of the refined simulations show that the grid refinement leads to somewhat sharper concentration fronts and a reduction of local oscillations (Figs. 8, 9, and 10).

However, a more detailed analysis of this aspect was not possible due to the substantial CPU-requirements associated with very fine discretizations. In the time available for this benchmarking project, only the code of Hoffmann et al. was able to compute a solution on such a fine mesh. Hence it was not possible to check this solution with a second code. For this reason, we cannot conclude if the three codes will converge to the same solution and we do not give an error norm because we did not get a reference solution.

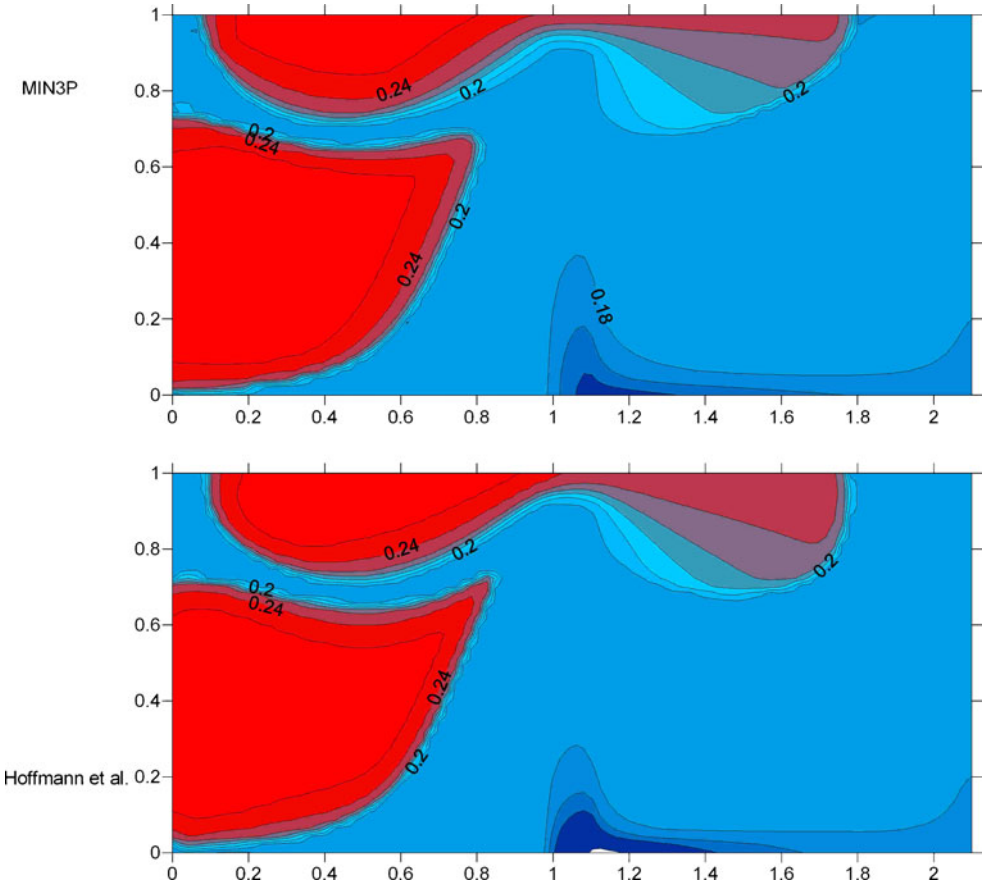

Fig. 9 Concentration contour maps for component X_3 at time 1,000 for the easy 2D advective test case (refined discretization, no CPU time constraint)

5.5 2D easy dispersive test case

The maximum allowed computing time for this case was set to 10,000 CPU units. This benchmark was only completed by two codes. The HYTEC simulation used 840 cells (42 × 20), and MIN3P employed a grid with 5,250 cells (105 × 50), the same discretization as for the 2D advective case.

The results are compared based on the concentration contour map of the immobile component S at time 10 (Fig. 11). S concentrations are depleted completely in the vicinity of the two injection locations, and a very thin and high amplitude S peak appears, similar to the results presented in Figs. 5 and 6 for the 1D easy advective test case. The simulation results from both codes indicate that these narrow and sharp peaks are difficult to resolve in a 2D simulation. A possible remedy would be grid refinement; however, this is difficult to achieve considering the extreme stiffness and high computational demand of this test problem.

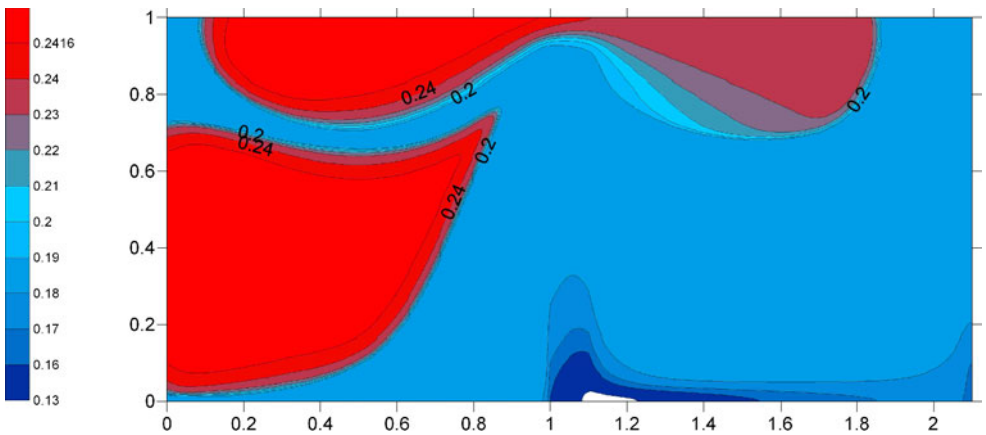

Fig. 10 Concentration contour maps for component X_3 at time 1,000 for the easy 2D advective test case calculated by Hoffmann et al. using a very fine mesh (608,256 cells)

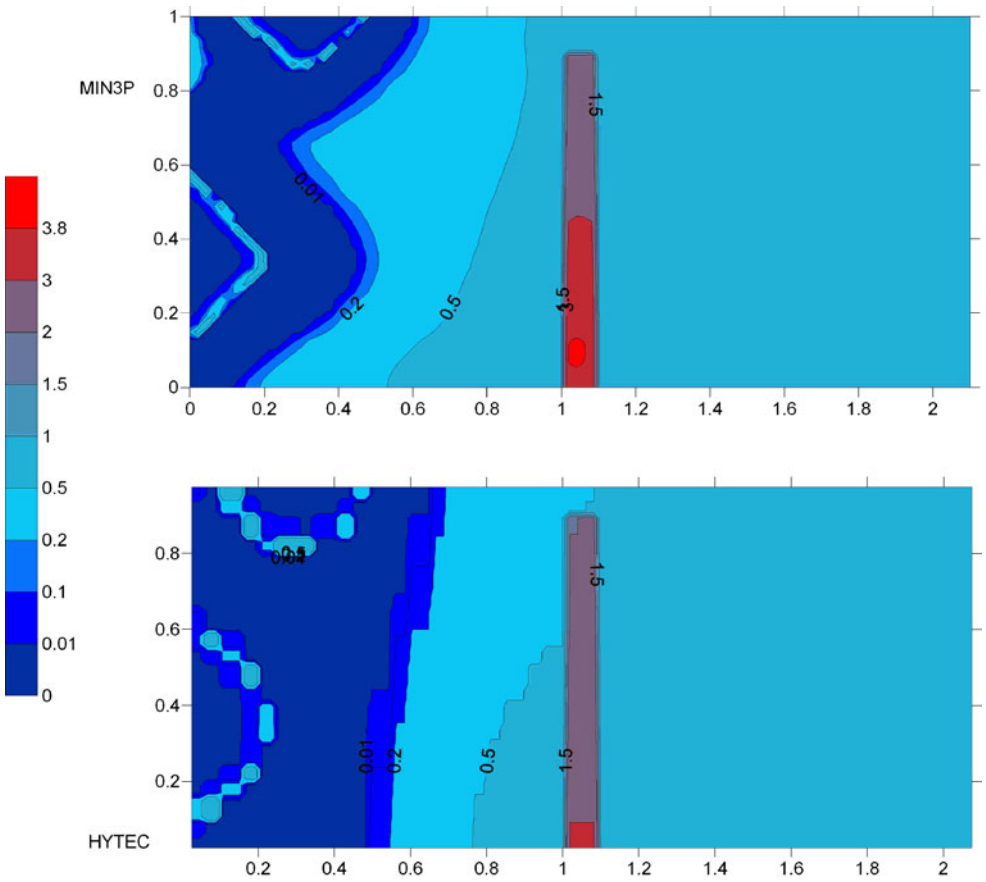

Fig. 11 Concentration contour maps of solid component S at time 10 for the 2D easy dispersive test case

Nevertheless, the results are encouraging in the sense that both simulations produce the same characteristic system behavior.

6 Synthesis of results

6.1 About the benchmark

The staged design of the benchmark was useful because it allowed comparing numerous methods and codes, independent of the level of development. Some of the established codes were able to tackle the benchmark on all three levels, while codes with a more limited reaction network could also participate. Using a fictitious chemical reaction network helped to focus on numerical issues and ensured that differences in the results are due to methods, algorithms, or implementations and not to discrepancies in the geochemistry databases. For the 2D cases, codes with parallel capabilities are needed to solve the problem accurately, i.e., to define a reference solution. Another possibility for future evaluation would be to make the problem "chemically easier" to allow for a quantitative comparison.

6.2 A good confidence in all methods

One of the main outcomes of this benchmark exercise is that the various methods used in this paper for solving reactive transport equations were able to solve the benchmark test cases and to capture their characteristic features both in time and space. Despite some localized differences, the simulation results are quite comparable, which builds confidence in the reactive transport modeling approach in general. Another outcome of this exercise is that some of the codes presented here have been improved to perform this benchmark.

6.3 About sequential approaches

Sequential approaches for reactive transport coupling are attractive because of their highest modularity and flexibility. Since models are becoming increasingly more complex, a modular and "library-based" approach, in which all libraries can be tested as independent modules, is strongly recommended (e.g., as implemented in HYTEC). The sequential approach allows for code development by a team of programmers working relatively independently. Indeed, this method breaks down the reactive transport problem naturally

into three major modules: chemistry, transport, and coupling. Moreover, they allow the use of any chemistry solver with all the knowledge of geochemistry databases. On the other hand, global methods require computing chemistry functions and derivatives and cannot use current chemistry solvers, which do not provide these interfaces. It is well known that operator splitting combined with a noniterative sequential approach (e.g., SPECY) introduces an a priori unknown error. This benchmark illustrates clearly that this method can be used with a rigorous control of errors.

6.4 About global methods

We show with our results that current global approaches can handle large systems describing 1D and 2D reactive transport. As a matter of fact, the simulations of the 2D benchmark were not limited by system memory but by computational time. For the test cases considered, global methods are very competitive in terms of computational efficiency, compared to sequential approaches.

We compared three codes implementing a global approach and using different primary unknowns. Because GDAE1D is based on a differential and algebraic system, it leads to the highest number of coupled unknowns (number of species plus number of components) per number of cells. In a direct substitution approach like in MIN3P, the number of coupled unknowns is reduced to the number of components per number of cells. The reduction scheme implemented by Hoffmann et al. uses even less coupled unknowns, reducing down to three decoupled components per number of cells plus two coupled components per number of cells. A comparison of the CPU time curves (Figs. 2, 3, and 4) illustrates the effect of reducing the number of unknowns. A new version of GDAE1D is under development, where a substitution approach is applied at the linear level. This allows keeping the nice features of DAE solvers with an adaptive time step based on error estimation and an adaptive control of convergence for nonlinear iterations.

6.5 Impact of the dominant transport phenomenon

We show here that all the numerical methods are able to give an accurate solution for both advective and dispersive cases. Nevertheless, it seems that the SNIA method is well adapted for advective problems, with a good tradeoff between accuracy, computational time, and ease of implementation. On the other hand, using the SNIA approach for a dispersive problem must be associated with an increase of the computing cost by reducing the time step or by refining the mesh. The SIA and global approaches are less dependent on the dominant transport phenomenon leading to a good accuracy for both advective and dispersive flows. This accuracy is obtained at the cost of the CPU time for SIA approaches and at the cost of the ease of implementation for global approaches.

6.6 About mesh and time refinement

Looking at Table 2, SPECY is the only code that does not use any adaptive time step. Computing time is lost to perform small time steps during the steady-state period (time between 3,000 and 5,000). An adaptive time step is a very important point to increase the efficiency of a reactive transport code without any loss of accuracy. Nevertheless, all codes compared here use some heuristic methods for time step adaptation based on the convergence rate of the linearization method. Only GDAE1D uses an adaptive order for time discretization and uses an error estimation computed in the DAE solver. This last feature can explain its high accuracy despite the coarse grids used. Further research on reactive transport codes should deal with adaptive time step strategies based on a predictor–corrector scheme or on error estimators.

Looking again at Table 2, some codes use a uniform grid, whereas some other codes refine the mesh in medium B. This mesh refinement reduces significantly computational time. None of the code uses adaptive mesh refinement. This is also a main perspective of research for reactive transport codes.

7 Conclusion and future work

A new benchmark has been designed to compare numerical methods for reactive transport models. This paper presents four different test cases, in 1D and 2D, with advective or dispersive transport conditions. Three classical methods for coupling have been used to solve this benchmark: SNIA with operator splitting (SPECY); SIA (HYTEC), DSA (MIN3P). In addition, two new mathematical methods have been proposed for the solution of reactive transport problems: a DAE approach (GDAE1D) and a reduction scheme (code of Hoffmann et al.). The use of a DAE solver provides an easy way to adapt the time step and to control convergence of Newton iterations, leading to accurate solutions. The reduction scheme presents an important innovation for this field of research, since it allows obtaining accurate solutions at a relatively low computational cost. Implementation of this reduction

scheme may also benefit other approaches. In the case of iterative fixed-point approaches, it could be a way of reducing the number of Picard iterations between chemistry and transport. In the case of noniterative approaches, the reduction method may help to control errors. These two points could be targets for future research.

The most important outcome of this benchmark exercise is that all approaches (SNIA, SIA, DSA, and DAE) were able to generate accurate results for problems of significant complexity and computational difficulty. This finding builds confidence in the use of reactive transport models to help in the assessment of environmental problems in earth sciences and engineering. It has also confirmed that various approaches have different advantages and disadvantages; therefore, a single superior method that is best for all problems cannot be identified. Nevertheless, the good performance of the relatively new code by Hoffmann et al., both in terms of relative accuracy and efficiency, highlights the need for continued collaboration between mathematicians, computer scientists, hydrogeologists, and geochemists.

The benchmark can also be used as a starting point for new comparison exercises. For example, simulations could be enhanced to address a limitation of the current tests. None of the current simulations provide a thorough test for analyzing the effect of transverse dispersion. This deficiency could be removed in the 2D version of the benchmark simply by modifying the boundary conditions to prescribe the injection of different solutions in each injection zone. Dissolved species contained within these solutions would mix along the flowpath and could react with each other subject to either equilibrium or kinetic reactions. In this context, various scenarios could be envisioned, in which the product of the mixing reaction precipitates (equilibrium, kinetically controlled), sorbs, or remains in solution. In addition, the number of components and species could be increased in order to be more representative of real-world reactive transport problems.

Acknowledgements This work has been supported by MoMaS CNRS-2439. We gratefully acknowledge sponsorship of GDR MoMAS by ANDRA, BRGM, CEA, EDF, and IRSN.

References

1. Bain, J.G., Mayer, K.U., Molson, J.W.H., Blowes, D.W., Frind, E.O., Kahnt, R., Jenk, U.: Assessment of the suitability of reactive transport modelling for the evaluation of mine closure options. J. Contam. Hydrol. **52**, 109–135 (2001)
2. Barry, D.A., Miller, C.T., Culligan-Hensley, P.J.: Temporal discretisation errors in non-iterative split-operator approaches to solving chemical reaction/groundwater transport models. J. Contam. Hydrol. **22**, 1–17 (1996)
3. Barry, D.A., Miller, C.T., Culligan, P.J., Bajracharya, K.: Analysis of split operator methods for nonlinear and multispecies groundwater chemical transport models. Math. Comput. Simul. **43**, 331–341 (1997)
4. Bauer, R.D., Rolle, M., Bauer, S., Eberhardt, C., Grathwohl, P., Kolditz, O., Meckenstock, R.U., Griebler, C.: Enhanced biodegradation by hydraulic heterogeneities in petroleum hydrocarbon plumes. J. Contam. Hydrol. **105**, 56–68 (2009)
5. Carnahan, C.L., Remer, J.S.: Nonequilibrium and equilibrium sorption with a linear sorption isotherm during mass transport through an infinite porous medium: some analytical solutions. J. Hydrol. **73**, 227–258 (1984)
6. Carrayrou, J.: Looking for some reference solutions for the reactive transport benchmark of MoMaS with SPECY. Comput. Geosci. (2010, this issue). doi:10.1007/s10596-009-9161-y
7. Carrayrou, J., Mosé, R., Behra, Ph.: A new efficient algorithm for solving thermodynamic chemistry. AIChE. J. **48**, 894–904 (2002)
8. Carrayrou, J., Mosé, R., Behra, Ph.: Modélisation du transport réactif en milieu poreux : schéma itératif associé à une combinaison d'éléments finis discontinus et mixtes-hybrides. Comptes Rendus Ac. Sci Mécanique **331**, 211–216 (2003)
9. Carrayrou, J., Mosé, R., Behra, Ph.: Efficiency of operator splitting procedures for solving reactive transport equation. J. Contam. Hydrol. **68**, 239–268 (2004)
10. Carrayrou, J., Kern, M., Knabner, P.: Reactive transport benchmark of MoMaS. Comput. Geosci. (2010, this issue). doi:10.1007/s10596-009-9157-7
11. de Dieuleveult, C.: Un modèle numérique global et performant pour le couplage géochimie-transport. Ph.D. thesis, University of Rennes 1 (2008)
12. de Dieuleveult, C., Erhel, J.: A global approach to reactive transport: application to the MoMaS benchmark. Comput. Geosci. (2010, this issue). doi:10.1007/s10596-009-9163-9
13. de Dieuleveult, C., Erhel, J., Kern, M.: A global strategy for solving reactive transport equations. J. Comput. Phys. **228**, 6395–6410 (2009)
14. De Windt, L., Burnol, A., Montarnal, P., van der Lee, J.: Intercomparison of reactive transport models applied to UO_2 oxidative dissolution and uranium migration. J. Contam. Hydrol. **61**, 303–312 (2003)
15. De Windt, L., Schneider, H., Ferry, C., Catalette, H., Lagneau, V., Poinssot, C., Poulesquen, A., Jegou, C.: Modeling spent nuclear fuel alteration and radionuclide migration in disposal conditions. Radiochim. Acta **94**, 787–794 (2006)
16. Fahs, M., Carrayrou, J., Younes, A., Ackerer, P.: On the efficiency of the direct substitution approach for reactive transport problems in porous media. Water Air Soil Pollut. **193**, 299–308 (2008)
17. Freedman, V.L., Ibaraki, M.: Coupled reactive mass transport and fluid flow: issues in model verification. Adv. Water Resour. **26**, 117–127 (2003)
18. Henderson, T.H., Mayer, K.U., Parker, B.L., Al, T.A.: Three-dimensional density-dependent flow and multicomponent reactive transport modeling of chlorinated solvent oxidation by potassium permanganate. J. Contam. Hydrol. **106**, 183–199 (2009)
19. Hoffmann, J., Kräutle, S., Knabner, P.: A parallel global-implicit 2-D solver for reactive transport problems in porous

media based on a reduction scheme and its application to the MoMAS benchmark problem. Comput. Geosci. (2010, this issue). doi:10.1007/s10596-009-9173-7
20. Kaluarachchi, J.J., Morshed, J.: Critical assessment of the operator-splitting technique in solving the advection–dispersion–reaction equation: 1. First-order reaction. Adv. Water Resour. **18**, 89–100 (1995)
21. Kanney, J.F., Miller, C.T., Kelley, C.T.: Convergence of iterative split-operator for approximating non-linear reactive transport problem. Adv. Water Resour. **26**, 247–261 (2003)
22. Kräutle, S., Knabner, P.: A new numerical reduction scheme for coupled multicomponent transport–reaction problems in porous media: generalization to problems with heterogeneous equilibrium reactions. Water Resour. Res. **43**, W03429.1–W03429.15 (2007). doi:10.1029/2005WR004465
23. Lagneau, V., van der Lee, J.: HYTEC results of the MoMas reactive transport benchmark. Comput. Geosci. (2010, this issue). doi:10.1007/s10596-009-9159-5
24. Leeming, G.J.S., Mayer, K.U., Simpson, R.B.: Effects of chemical reactions on iterative methods for implicit time stepping. Adv. Water Resour. **22**, 333–347 (1998)
25. Maher, K., Steefel, C.I., White, A.F., Stonestrom, D.A.: The role of reaction affinity and secondary minerals in regulating chemical weathering rates at the Santa Cruz Soil Chronosequence, California. Geochim. Cosmochim. Acta **73**, 2804–2831 (2009)
26. Mayer, K.U., MacQuarrie, K.T.B.: Solution of the MoMaS reactive transport benchmark with MIN3P–model formulation and simulation results. Comput. Geosci. (2010, this issue). doi:10.1007/s10596-009-9158-6
27. Mayer, K.U., Benner, S.G., Frind, E.O., Thornton, S.F., Lerner, D.L.: Reactive transport modeling of processes controlling the distribution and natural attenuation of phenolic compounds in a deep sandstone aquifer. J. Contam. Hydrol. **53**, 341–368 (2001)
28. Mayer, K.U., Frind, E.O., Blowes, D.W.: Multicomponent reactive transport modeling in variably saturated porous media using a generalized formulation for kinetically controlled reactions. Water Resour. Res. **38**, 1174 (2002). doi:10:1029/2001WR000862
29. Mayer, K.U., Benner, S.G., Blowes, D.W.: Process-based reactive transport modeling of a permeable reactive barrier for the treatment of mine drainage. J. Contam. Hydrol. **85**, 195–211 (2006)
30. Molinero, J., Samper, J.: Large-scale modeling of reactive solute transport in fracture zones of granitic bedrocks. J. Contam. Hydrol. **82**, 293–318 (2006)
31. Molins, S., Mayer, K.U.: Coupling between geochemical reactions and multicomponent gas diffusion and advection—a reactive transport modeling study. Water Resour. Res. **43**, W05435 (2007). doi:10.1029/2006WR005206
32. Nowack, B., Mayer, K.U., Oswald, S.E., Van Beinum, W., Appelo, C.A.J., Jacques, D., Seuntjens, P., Gerard, F., Jaillard, B., Schnepf, A., Roose, T.: Verification and intercomparison of reactive transport codes to describe root-uptake. Plant and Soil **285**, 305–321 (2006)
33. Prommer, H., Aziz, L.H., Bolaño, N., Taubald, H., Schüth, C.: Modelling of geochemical and isotopic changes in a column experiment for degradation of TCE by zero-valent iron. J. Contam. Hydrol. **97**, 13–26 (2008)
34. Reeves, H., Kirkner, D.J.: Multicomponent mass transport with homogeneous and heterogeneous chemical reactions: effect of the chemistry on the choice of numerical algorithm. 2. Numerical results. Water Resour. Res. **24**, 1730–1739 (1988)
35. Saaltink, M.W., Carrera, J., Ayora, C.: A comparison of two approaches for reactive transport modelling. J. Geochem. Explor. **69–70**, 97–101 (2000)
36. Saaltink, M.W., Carrera, J., Ayora, C.: On the behavior of approaches to simulate reactive transport. J. Contam. Hydrol. **48**, 213–235 (2001)
37. Salvage, K.M., Yeh, G.T.: Development and application of a numerical model of kinetic and equilibrium microbiological and geochemical reactions (BIOKEMOD). J. Hydrol. **209**, 27–52 (1998)
38. Selim, H.M., Mansell, R.S.: Analytical solution of the equation for transport of reactive solutes through soils. Water Resour. Res. **12**, 528–532 (1976)
39. Shen, H., Nikolaidis, N.P.: A direct substitution method for multicomponent solute transport in ground water. Ground Water **35**, 67–78 (1997)
40. Siegel, P., Mosé, R., Ackerer, Ph., Jaffre, J.: Solution of the advection–diffusion equation using a combination of discontinuous and mixed finite elements. Int. J. Num. Methods Fluids **24**, 595–613 (1997)
41. Spiessl, S.M., MacQuarrie, K.T.B., Mayer, K.U.: Identification of key parameters controlling dissolved oxygen migration and attenuation in fractured crystalline rocks. J. Contam. Hydrol. **95**, 141–153 (2008)
42. Steefel, C.I., Lasaga, A.C.: A coupled model for transport of multiple chemical species and kinetic precipitation/dissolution reactions with application to reactive flow in single phase hydrothermal systems. Am. J. Sci. **294**, 529–592 (1994)
43. Steefel, C.I., MacQuarrie, K.T.B.: Approaches to modelling of reactive transport in porous media. In: Lichtner, P.C., Steefel, C.I., Oelkers, E.H. (eds.) Reactive Transport in Porous Media, vol. 34, pp. 82–129. Reviews in Mineralogy, Mineralogical Society of America, Washington (1996)
44. Steefel, C.I., Carroll, S., Zhao, P.H., Roberts, S.: Cesium migration in Hanford sediment: a multisite cation exchange model based on laboratory transport experiments. J. Contam. Hydrol. **67**, 219–246 (2003)
45. Sun, Y., Petersen, J.N., Clement, T.P.: Analytical solutions for multiple species reactive transport in multiple dimensions. J. Contam. Hydrol. **35**, 429–440 (1999)
46. Toride, N., Leij, F.J., van Genuchten, M.T.: A comprehensive set of analytical solutions for nonequilibrium solute transport with first-order decay and zero-order production. Water Resour. Res. **29**, 2167–2182 (1993)
47. Valocchi, A.J., Malmstead, M.: Accuracy of operator-splitting for advection–dispersion–reaction problems. Water Resour. Res. **28**, 1471–1476 (1992)
48. van Genuchten, M.T.: Analytical solutions for chemical transport with simultaneous adsorption, zero-order production and first-order decay. J. Hydrol. **49**, 213–233 (1981)
49. van Genuchten, M.T., Wierenga, P.J.: Mass transfer studies in sorbing porous media. 1. Analytical solutions. Soil Sci. Soc. Am. J. **40**, 473–480 (1976)
50. van Genuchten, M.T., Wierenga, P.J., O'Connor, G.A.: Mass transfer studies in sorbing porous media. 3. Experimental evaluation with 2,4,5-T[1]. Soil Sci. Soc. Am. J. **41**, 278–285 (1976)
51. van der Lee, J., De Windt, L., Lagneau, V., Goblet, P.: Module-oriented modeling of reactive transport with HYTEC. Comput. Geosci. **29**, 265–275 (2003)
52. van der Lee, J., Langeau, V.: Rigorous methods for reactive transport in unsaturated porous medium coupled with chemistry and variable porosity. In: Miller, C.T.,

Farthing, M.W., Gray, W.G., Pinder, G.F. (eds.) Computational methods in water resources (CMWR XV), vol. 48(1), pp. 861–868. Elsevier (2004)
53. Walter, A.L., Frind, E.O., Blowes, D.W., Ptacek, C.J., Molson, J.W.: Modelling of multicomponent reactive transport in groundwater, 2. Metal mobility in aquifers impacted by acidic mine tailings discharge. Water Resour. Res. **30**, 3149–3158 (1994)
54. Yeh, G.T., Tripathi, V.S.: A critical evaluation of recent developments in hydrogeochemical transport models of reactive multichemical components. Water Resour. Res. **25**, 93–108 (1989)